ISSN 1330-3651 (Print), ISSN 1848-6339 (Online)
https://doi.org/10.17559/TV-20230504000606
Original scientific paper

# The Effect of Channel Depth on Joint Quality in Cu/AISI 1040 Materials Joined by Mechanical Locking Method

Serdar MERCAN*, Arslan KAPTAN*

**Abstract:** The aim of this study is to investigate a novel and environmentally friendly method that is an alternative to conventional methods in the production of bi-metallic products. Bi-metallic products are obtained by joining materials with different physical and chemical properties. As a result, the desired properties of different materials can be used together. Numerous conventional methods such as welding, casting and pressing are used in the production of bi-metal materials. However, Cu and AISI 1040 steel materials are almost impossible to be joined by conventional production methods. The original value of this study is that these materials can be joined by a new method, the Mechanical Locking Method. In the joining process, a constant speed (1400 rpm), a constant feed rate (16 mm/min) and different channel depths (10, 13, and 15 mm) were used. The effect of the channel depth, one of the physical design parameters, on the joint quality was investigated. The mechanical and microstructural properties of the joint were determined experimentally. In conclusion, it was determined that the Cu/AISI 1040 material pair was successfully joined by using the Mechanical Locking Method and the most suitable channel depth was 10 mm.

**Keywords:** friction; mechanical locking method; mechanics; microstructure; plastic deformation

## 1 INTRODUCTION

Bi-metallic products are fabricated by joining materials with different physical and chemical properties using various methods. Welding and casting from these methods are not always suitable for dissimilar materials. The Mechanical Locking Method (MLM), working based on the principle of joining materials through plastic deformation, is an alternative, environmentally friendly and novel method. This method is used to join different metal pairs such as copper and steel or aluminium and steel and also join metals with non-metallic materials such as ceramics. Thus, different types of materials can be used together. These bi-metallic applications bring the desired mechanical and financial advantages of each material type together.

In the Mechanical Locking Method, a part with high mechanical properties is designed as mold part (MP) and the other as reshaped part (RP) among the parts to be joined. There is a system designed to ensure the friction of RP at the interface in the conical channel drilled on MP. Due to sufficient heat obtained as a result of friction as well as increasing axial force pressure, RP joint metal is accumulated in the channel through plastic deformation [1]. Thus, the joint is achieved in a closed mold through deformation similar to the hot forging process and by converting mechanical energy into thermal energy [2]. This produces a non-detachable joint. The friction and upset pressures used in this method are similar to those in the friction welding method. The flanges forming during the joining process in the friction welding method are used for the joint in MLM. The use of waste flanges in joining processes brings out the environmentalist aspect of the method. There is no need for additional filling material in joining processes, as in welding and adhesion methods. No waste or slag forms after joining. It is a method suitable for mass production. The method can be used in industrial applications such as the production of thermal contacts, thermostats, crusher hammers, and decorative products. On the other hand, the most important disadvantages of the method are that the materials to be joined require preliminary preparation and there is a need for a table depending on the size of the pieces.

Copper (Cu), designed as RP in this study, is preferred for explosive-flammable environments due to the fact that it is high corrosion resistant and it has a paramagnetic [3, 4] and non-sparking structure. It is a metal type whose alloys have high mechanical properties and are suitable for plastic deformation. Heat treatment is not applied and it features hardening as a result of cold forming. The thermal conductivity of copper is very high compared to steel types. It has a wide range of application areas together with steel. Copper and steel-based material pairs benefit from their thermal and electrical properties in pipe joints to avoid unwanted heating in cooling systems [5]. When the studies on the joining of copper and steel pairs by welding and casting are examined, it is seen that unstable joining and irregular morphology at the interface form [6] and mechanical strength reduces [7] in the joining process. In fact, it is known that high stresses and consequential damage [8] occur depending on welding defects even in welded joints of dissimilar steels. Due to the difference in the thermal expansion coefficients of copper and steel, cracks occur in the weld zone [9] and the weld strength of Cu/AISI 304 L austenitic stainless steel joined by friction welding method is weakened at the interface due to the presence of intermetallic layers [10, 11]. The analysis of the welded joint in these materials joined by the diffusion welding method confirmed the theoretical fracture conditions [12]. Previous studies have reported that it is difficult to join copper-steel by laser welding [13]; cracks occur in the intermetallic layers of copper-steel tubes joined by electromagnetic welding [14], strength incompatibility is seen in copper-steel joined by hot isostatic pressing [15], the coarse grain region forms the weak point in the joining of Cu and AISI 304 through electron beam welding [16], and differences in the physical and chemical properties of the materials make welding processes difficult [17]. Since the joint is not atomic in MLM, these problems are eliminated.

The successful applicability of MLM, which was developed to eliminate the disadvantages of conventional joining methods, was supported by experimental studies within the scope of this study. A comprehensive study on joining of Cu/AISI 1040 materials by this novel and

environmentally friendly method has not been carried out so far. Therefore, we think that this study would make significant contributions to the literature.

## 2 MATERIAL AND METHOD

### 2.1 Experiment

The melting temperature and strength of AISI 1040 steel to be joined using MLM are higher than those of Cu. Therefore, AISI 1040 material was designed as MP and Cu material was designed as RP. MP and RP were fabricated on a CNC machine in accordance with the determined physical design criteria. A Taksan FU 315 × 1250 V/2 milling machine was used for the friction of the samples along the contact line and the required axial pressure. Fig. 1a shows the schematic view of the experiment and Fig. 1b shows the experimental procedure. During the experiment, AISI 1040 material was fixed on the machine table and Cu was fixed to the rotary head with a clamp. Although the melting temperature of Cu is about 1100 °C, Cu melts at about 1400 °C due to the formation of copper oxide on its outer surface. This requires more heat formation for the plastic deformation on its outer surface layer. The researcher waited for 10 s to provide temperature increase by friction after the contact of the samples at the interface. Then, the machine was operated at a constant feed rate until the desired plastic deformation process was completed. At the end of the process, the machine was suddenly stopped to prevent possible micro-welded areas from being ruptured. The heat obtained by converting the mechanical energy, releasing through friction, into thermal energy was used at the interfaces of the samples. The RP, plasticized by the axial pressure, was shaped appropriately in the conical channel of MP. A mechanical joint was achieved with a narrow heat-affected zone (HAZ) without using any additional material throughout the process.

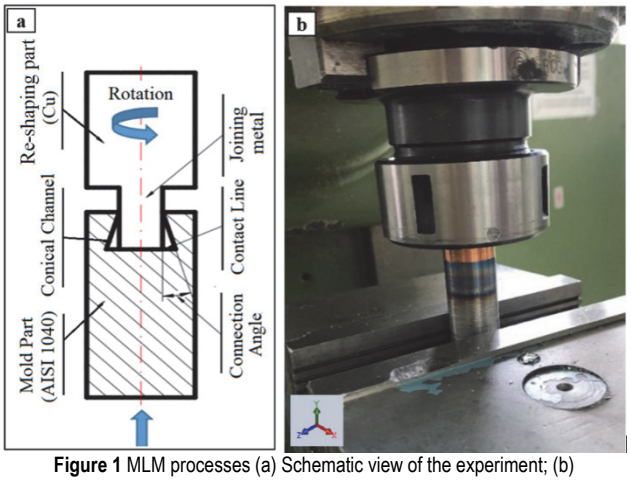


**Figure 1** MLM processes (a) Schematic view of the experiment; (b) Experimental procedure

The joined samples were machined on the milling machine by the machining method using the coolant up to the axis of symmetry. Then, they were gradually ground with 150-2500 grit sandpaper. 3-µm and then 1-µm diamond paste was used to polish them. The steel side was etched with 1% nitric acid and the copper side with 2% hydrofluoric acid. After macro photos were analysed, the microstructures in the joint zone were evaluated with Tescan Mira3XMU SEM device.

Microhardness values were measured to the matrix from three directions (a, b and c) shown in Fig. 2 in the axial direction perpendicular to the contact line at the interface of the cross-sectioned samples. The Vickers hardness measurements were completed using HV-2000 Schimadzu device under 1 kg-f load, with 1 mm intervals and for a waiting time of 15 s.

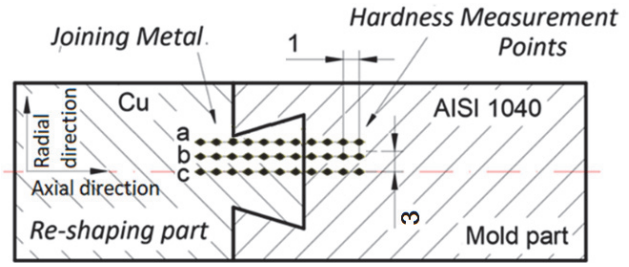


**Figure 2** Microhardness measuring / mm

The samples were subjected to tensile tests. Their mechanical test results were compared. The tests were completed in Instron 5982 test machine using an extensometer at a strain rate of $1 \times 10^{-3}$ $s^{-1}$. For better comparison, the mechanical properties of the base material (Cu) were identified by preparing a tensile sample in accordance with DIN 50 125 standards. Fig. 3 shows the tensile test sample of Cu and the damaged part at the end of the experiment.

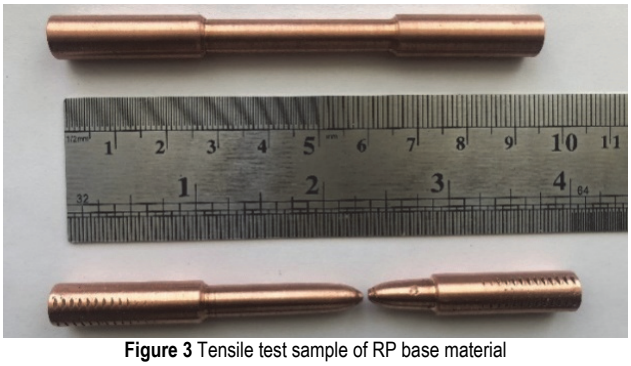

**Figure 3** Tensile test sample of RP base material

### 2.2 Joining Parameters

The heat obtained as a result of friction had a significant effect on the amount of the material that was subjected to plastic deformation and on the material flow, which affects the quality of the joint. Many results such as the microstructure of the joint area, the defects in the joint and the extent of these defects vary depending on the heat and material flow. Therefore, the heat must be selected at a sufficient level to allow material flow, which is directly correlated with rpm as reported by the studies [17]. Given the joining time in the preliminary tests, the experiments were completed at a constant speed (1400 rpm). In each sample, the parts were subjected to friction for 10 s before the feed motion and thus the heat increased.

The feed rate would cause axial pressure. Hence, it is needed to allow sufficient material flow at plastic deformation temperature, without any buckling since the heat produced on the friction materials reduces rapidly while the materials move away from the friction zone by forming a flange [18], so the temperature rises on the face-to-face friction surfaces of the two materials. The RP (Cu)

material becomes doughy, forms a flange and moves into the channel while leaving the friction interface under the effect of axial pressure, and thus begins to cool rapidly outside the contact surface. Therefore, a layer of material, which has not yet become dough and has a lower temperature, comes out at the friction interface. Temperature to increase requires a time in order to include this layer in the flange. If the feed rate is kept too high at this stage, the Cu material with a narrow cross-section in the conical channel is buckled. Therefore, considering the preliminary experiments carried out in the light of the literature, the feed rate was set as 16 mm/min.

Cu and AISI 1040 materials shown schematically in Fig. 4 were provided as Ø24 × 175 mm. They were machined on CNC turning lathe in the dimensions specified in Tab. 1. The channel depth (h) examined in the study was prepared in 3 dimensions.

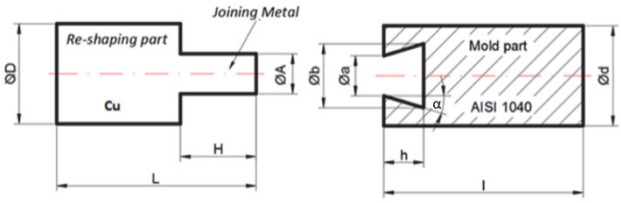


**Figure 4** Sample dimensions

**Table 1** Dimensions of the samples

| | | *S*1 | *S*2 | *S*3 |
|---|---|---|---|---|
| Mold Part (AISI 1040) | Channel depth (*h*) / mm | 10 | 13 | 15 |
| | Channel base diameter (*Øb*) / mm | 18.36 | 19.97 | 21.04 |
| | Nominal diameter (Ød) / mm | 24 | | |
| | Length (*l*) / mm | 75 | | |
| | Connection angle (*α*) / ° | 15 | | |
| | Channel mouth diameter (*Øa*) / mm | 13 | | |
| Reshaping Part (Cu) | Nominal diameter size (*ØD*) / mm | 24 | | |
| | Length (*L*) / mm | 100 | | |
| | Joint metal diameter (*ØA*) / mm | 13 | | |

As shown in Fig. 4, the channel mouth diameter (*a*) of the mold part was 13 mm (Tab. 1) and all samples were machined with a joining angle (*α*) of 15°. To calculate the volume of the joint metal at RP, the volume of the conical channel was determined using Eq. (1).

$$V = \int_0^h \pi \left[ \left( \frac{\frac{b}{2} - \frac{a}{2}}{h} \right) x + \frac{a}{2} \right]^2 \mathrm{d}x \Rightarrow V = \left( \frac{\pi h}{\frac{b}{2} - \frac{a}{2}} \right) \left( \frac{b^3 - a^3}{24} \right) \quad (1)$$

The height of the joint metal (*H*) to fill the frustum volume of Cu in the mold cavity was calculated by Eq. (2).

$$H_{\mathrm{Cu}} = \frac{V}{\pi \cdot \left( \frac{A}{2} \right)^2} \quad (2)$$

RP parts based on the equation were manufactured but no successful results were obtained in preliminary tests. The samples were damaged due to the joint metal compressed in the mold as a result of thermal expansion. Therefore, the height values ($H_{\mathrm{Cu}}$) of the joint metal were gradually reduced and it was manufactured as smaller than 0.5 mm and successful results were obtained. Tab. 2 shows the length and volume of the joint metal on Cu and Fig. 5 shows the prepared samples.

**Table 2** Dimensions of the joint metal

| Channel depth (*h*) / mm | 10 | 13 | 15 |
|---|---|---|---|
| Channel mouth diameter (*Øa*) / mm | 13 | | |
| Channel base diameter (*Øb*) / mm | 18.36 | 19.97 | 21.04 |
| Volume of Conical channel (*V*) / mm$^3$ | 1949.1 | 2815.4 | 3253.8 |
| Height of joint metal ($H_{\mathrm{Cu}}$) / mm | 14.7 | 21.2 | 26.2 |

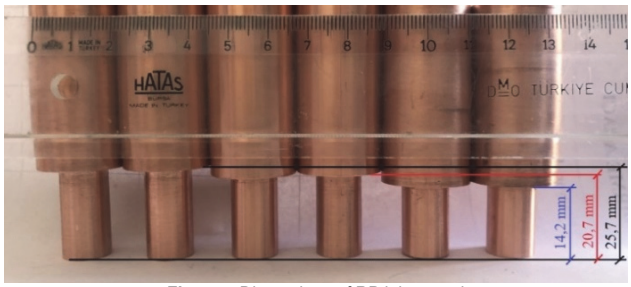


**Figure 5** Dimensions of RP joint metal

## 2.3 Material Properties

The chemical compositions of the materials were determined by spectral analysis and presented in Tab. 3. Tab. 4 shows the mechanical properties of this material pair.

**Table 3** Chemical composition of Cu and AISI 1040 material pair (wt.%)

| | C | Mn | Si | Cu | S | Ag | P | Fe |
|---|---|---|---|---|---|---|---|---|
| Cu | - | - | - | Bal | - | 0.002 | 0.09 | - |
| AISI 1040 | 0.42 | 0.55 | 0.30 | - | 0.03 | - | - | Bal. |

**Table 4** Physical properties of Cu and AISI 1040 material [19]

| Physical property | Cu | AISI 1040 |
|---|---|---|
| Density / × 1000 kg/m$^3$ | 8.94 | 7.84 |
| Modulus of Elasticity / MPa | 132 | 200 × 103 |
| Tensile Strength / MPa | 300 | 500-620 |
| Poisson Ratio | 0.35 | 0.28 |
| Yield Strength / MPa | 140 | 415 |
| Coefficient of Thermal Expansion / µm/m°C | 340 | 11.3 |
| Thermal Conductivity Coefficient / W/mK | 401 | 16.2 |
| Melting Temperature / °C | 1083 | 1454 |

# 3 RESULTS

## 3.1 Macrostructure Examination

In samples joined by MLM, a relative motion occurred between the contact surfaces of the parts by rotating one part. The axial pressure caused local temperature increases, as well. These events were repeated until a thermal equilibration took place on all contact surfaces in a very short time through thermal conduction [20]. The plasticized material, forming a flange ring, was provided by new flanges forming by the material flowing throughout the channel. After the relative motion was stopped, it compressed in the mold part and took the shape of the channel geometry. Fig. 6 shows a macro photo of the molded samples. The HAZ forming as a result of friction was more pronounced and wider on the side of AISI 1040

due to the greater difference between the thermal conductivity coefficients of the joined metals and the physical design of the joint. Since the conical channel on the AISI 1040 side and the Cu joint metal were shaped by friction on these channel surfaces, a wider HAZ on the side of AISI 1040 is an expected consequence. This actually indicates that the HAZ affected the whole of the joint metal.

The channel depth was 10, 13, and 15 mm in the samples *S*1, *S*2, and *S*3, respectively. HAZ expanded in each sample based on the increasing channel depth due to the increase in the heat generating depending on the machining time as a result of the increase in the channel depth. It is known that although the increased channel depth increases the load-bearing cross-section in the joint, it also increases the negative effect of HAZ on the materials.

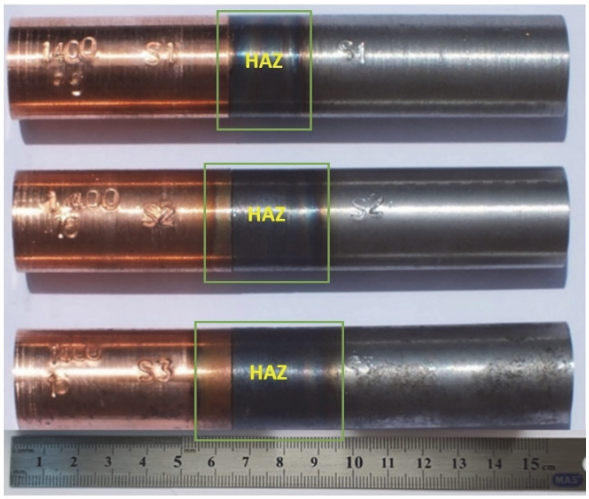


**Figure 6** Macro photos of the sample *S*1, *S*2, and *S*3

The interfacial macro photographs of the samples showed that all of the plastic deformations occurred on the Cu side as expected (Fig. 7). The lower melting temperature and mechanical properties of Cu were the determinant effects for the deformation zone [21]. During the plastic deformation process, porosities occurred in all three samples due to material flow (Fig. 7). This is due to the fact that the flanges forming the joint metal rapidly cooled down while moving away from the friction interface and the desired flow cannot be achieved. Porosities were visible at the corners of the samples *S*1 and *S*3 and in the inner parts of the sample *S*2. The interruptions of the flange flow due to various reasons and the dense mixture caused by the high rotational speed were the main causes of the formation of porosities at different points.

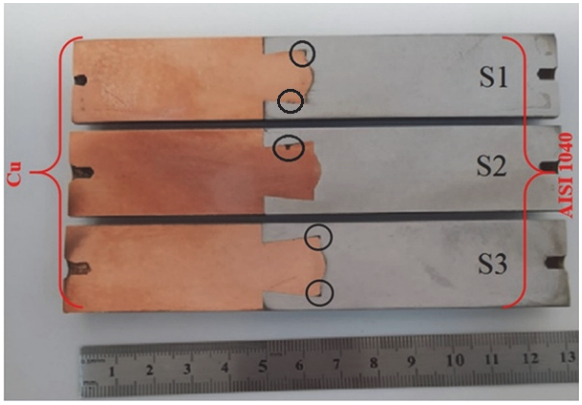


**Figure 7** Macro photos of the Interface

The samples were progressively machined in 1 mm passes up to the symmetry axis on the milling machine in order to examine the distribution of porosities on the joint metal in detail. The interface macro photos of the sample S1 (Fig. 8) show the porosities on the surfaces machined from 8 mm to 12 mm (symmetry axis). The porosities appeared in different sizes and different regions at each stage. These porosities were mainly due to the fact that the Cu material tended to form a circular flange with the pressure effect, as in friction welding, and thus the material flow to the sharp corners cannot be fully achieved. They formed at different points due to a high rotational speed, a dense mixing, and an irregular flow.

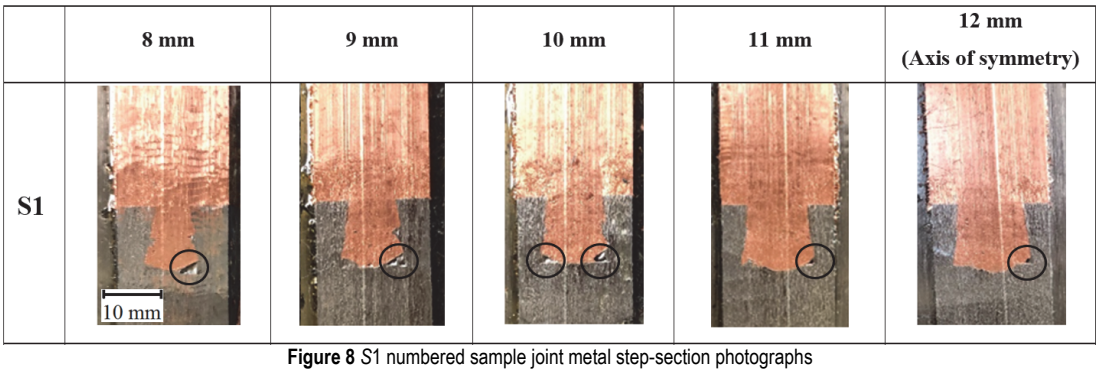


**Figure 8** *S*1 numbered sample joint metal step-section photographs

It has been reported in the literature that in the joining of dissimilar materials by MLM, cracks appear in the region where the cross-section becomes narrower and damage processes begin [22]. However, it was found that there were no micro and macro cracks in those zones in the Cu/AISI 1040 material pair. This was considered to be caused by the lower rates of thermal expansion and shrinkage depending on the high plastic deformation capability and high thermal conductivity coefficient of Cu.

However, the differences in thermal expansion coefficients make it very difficult to weld Cu and AISI 1040 material pair without any crack [9]. The cracks adversely affect the damage processes of the welded joints and bring the safety perception into the foreground. It is considered that safer joints can be achieved in MLM compared to other joining methods when the parameters and physical design variables are harmonized with each other in the investigations due to the low heat input used in MLM.

### 3.2 Microstructure Examination

Fig. 9 shows SEM images of friction and joint interfaces of all three samples. SEM images clearly show some porosities that were not identified in macro photos. The regions with porosity on RP (Cu) in all three samples were marked. In the literature, it has also been reported that insufficient thermal and metal flow in friction stir welding causes porosity in the stirring zone [23]. Similarly, insufficient/incompatible heat and axial pressure caused these porosities. The flanges moving away from the friction interface and progressing in the conical channel lose heat rapidly, which makes the movement of the following flanges difficult. This is confirmed by the relatively less amount of porosity in the sample *S*3, where more heat is generated compared to the samples *S*1 and *S*2 (Figs. 7, 8, and 9). On the other hand, the structural complexity caused by the corner points for material flow caused porosity in these regions of all three samples. However, it was clearly determined that increased channel depth increased the amount of porosity for the corner points. The expansion and shrinkage amount of the copper material clearly increased due to the high thermal cycle caused by the increased channel depth.

As a result, the cavities forming at the friction interface where the heat peaked were 0.2, 0.6, and 1.1 mm in the samples *S*1, *S*2, and *S*3, respectively. Increasing channel depth increased larger defective area. Shrinkage in the joint metals forming the side surfaces in all three samples was at similar rates since these surfaces were composed of relatively colder flange layers.

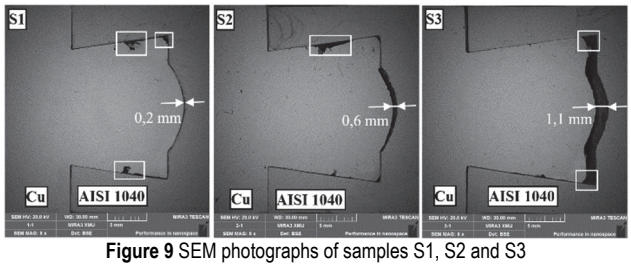


**Figure 9** SEM photographs of samples S1, S2 and S3

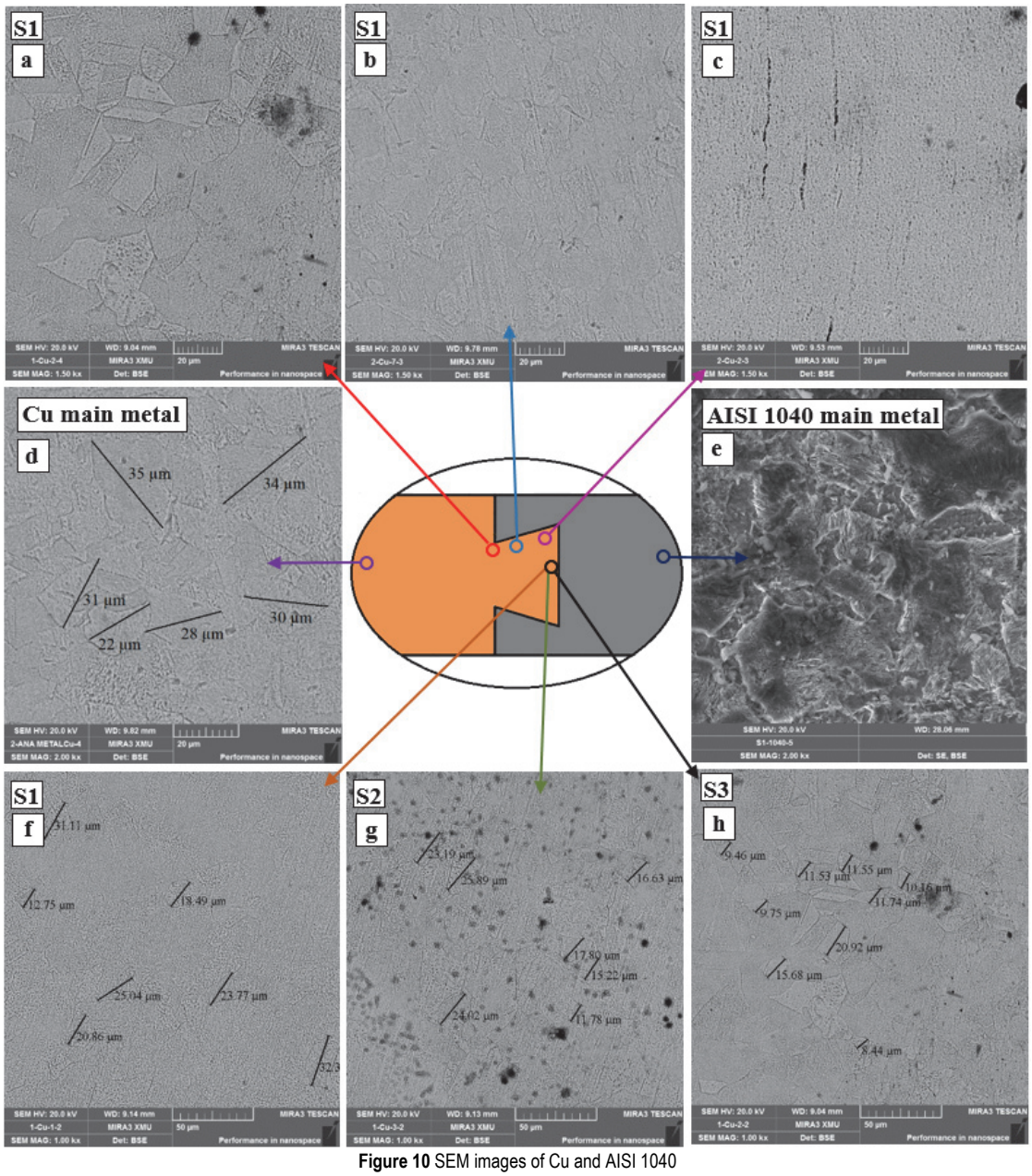


**Figure 10** SEM images of Cu and AISI 1040

Figs 10a, b, and c show SEM images taken from different points of the joint metal (Cu) in the sample *S*1. Fig. 10a shows that its microstructure was very close to the base metal microstructure. Fig. 10b shows that its microstructure was partially smaller than the base metal and was composed of grains orientated due to pressure. Fig. 10c, shows grains that were excessively subjected to plastic deformation and orientated. The thermal cycles at points a and b were sufficient for the Cu material to regain its original grain structure. However, the flanges forming the joint metal at point c were the last flanges. Since there were no other flanges that followed the last flanges, rapid cooling and sudden solidification caused the grains to form a finer structure. Similar results were observed in the other samples.

Figs. 10d and e show SEM images of Cu and AISI 1040 base metal. The average grain size of Cu was measured as 30 µm. Figs. 10f, g, and h show SEM images of the samples *S*1, *S*2, and *S*3 taken from the same point. In all three samples, the grain sizes consisted of smaller grains depending on the increasing channel depth. The average grain sizes were 23.47, 19.21, and 12.14 µm, respectively. This difference between the grain sizes was caused by the thermal cycles described above.

Fig. 11 shows detailed (100, 50, and 20 µm) SEM images of the sample *S*3. The images clearly show the grain orientations caused by plastic deformation.

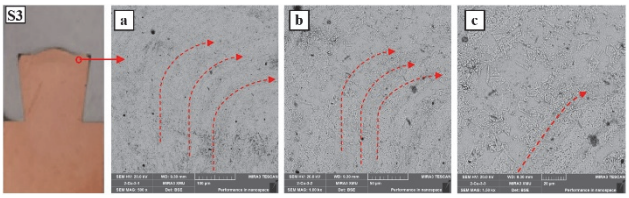


**Figure 11** SEM image of the sample S3 a) 100 µm; b) 50 µm; c) 20 µm

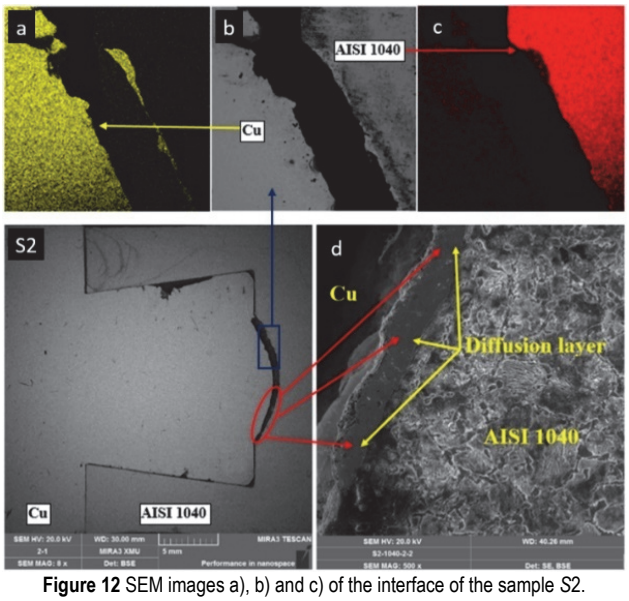


**Figure 12** SEM images a), b) and c) of the interface of the sample *S*2. Elemental change d) Diffused Cu material

In MLM, high diffusion between material pairs is not expected due to the joint design. However, some diffusion is possible with the effect of heat and pressure. Fig. 12 shows SEM images of the regions with diffusion in the sample *S*2. In the marked areas in the images (Fig. 12d), the material diffused from Cu to the AISI1040 side was seen as a layer. Diffusion was more intense at the friction interfaces compared to the other surfaces (Figs. 12a, b, and c). Despite the varying heat amount, it was determined that the diffusion was similar in the samples *S*1 and *S*2, and a partial increase was observed in the sample *S*3. This was caused by the rapid removal of the heated material from the interface.

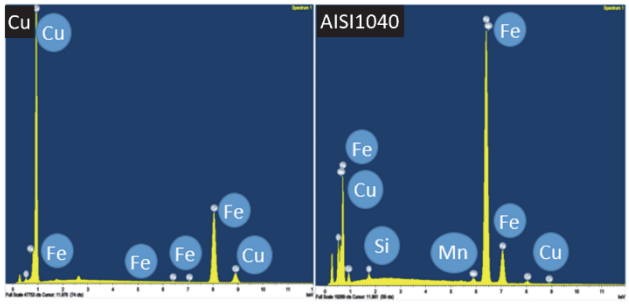


**Figure 13** EDX analysis of the sample *S*2

Fig. 13 shows the EDX analysis done on the sample S2 to determine the diffusion rate. The amount of mutual diffusion between both materials was low and partial. AISI 1040 material contained a low amount of Cu material due to diffusion.

### 3.3 Microhardness Measurement

The mean hardness values of the base material were measured as 186 and 404 HV for Cu and AISI 1040, respectively. Fig. 14 shows the microhardness measurements in three directions (a, b, and c). The hardness in the joint zone was inhomogeneous as stated in the literature [24].

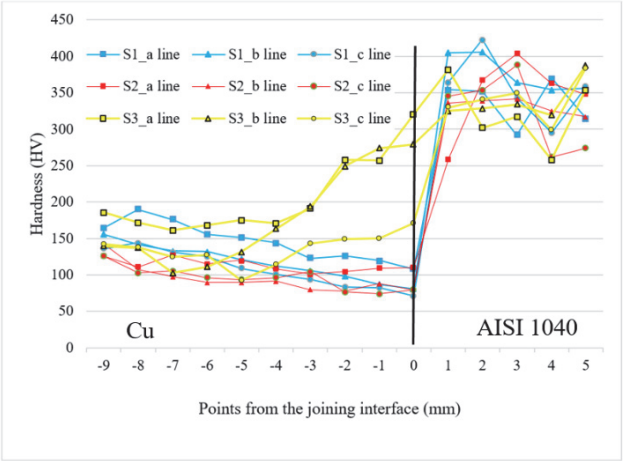


**Figure 14** Microhardness distributions of the samples *S*1, *S*2, and *S*3

In all three samples, there was no significant change in the hardness value on the AISI 1040 side compared to the base material. The slight reduction observed especially in the sample *S*3 was caused by the increased Cu diffusion due to high temperature.

On the side of Cu, the hardness value was close to the hardness of the base material approximately 8 mm after the friction interface in the channel. In general, it has been reported in the literature that a change in the hardness profile is caused by thermal cycles depending on the joining parameters [25]. Depending on the thermal input, it

was clearly noticed that the hardness values measured in three directions on the side of Cu in the samples *S*1 and *S*2 were close to each other and reduced slightly compared to the base material. This reduction persisted as it was getting closed to the friction interface. The reduction in hardness was caused by recrystallization process. In the sample *S*3, the hardness of the joint metal increased as it was getting closed to the friction interface. The heat on the joint metal, which was excessively subjected to plastic deformation, in the same sample was higher than the heat of the other samples. Therefore, the orientated fine grain structure in the microstructure forming by the flanges (Fig. 11), the higher mixture compared to the other samples and the diffusion of AISI 1040 material into some Cu material due to the rising heat as stated in the literature increased the hardness values [9].

### 3.4 Results of Mechanical Test

Fig. 15a shows macro images of the parts which were joined by MLM and damaged as a result of the tensile test in this study. Fig.15b shows results of the tensile test.

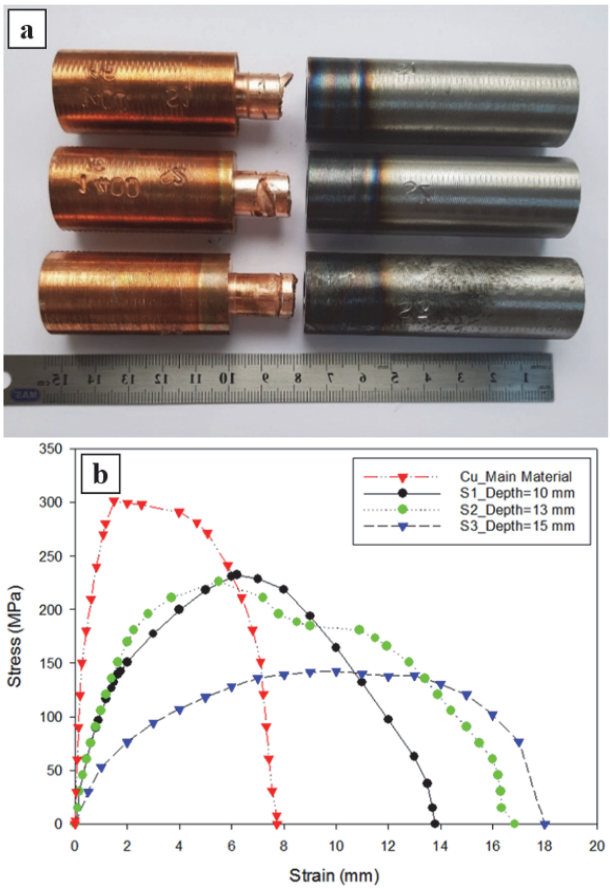


**Figure 15** Tensile test results a) Macro photo of tensile test results; b) Tensile test results

Damage on the Cu side, having lower tensile strength, is an expected outcome. Previous studies have reported that the damage is associated with fracture in the region where the cross-section becomes narrower [26]. However, the damage in all three samples joined in the study was not associated with fracture, but removal of the Cu sample out of the channel (Fig. 15a). The time for the complete removal of the joint metal from the mold varied in parallel with the depth of the channel.

The lowest stress value was obtained as 138 MPa in the sample *S*3 and the highest stress value was obtained as 236 MPa in the sample *S*1 (Fig. 15b). It was determined that the mechanical properties of the three samples degraded by approximately 22%, 27% and 54%, respectively, based on the base material's tensile strength (301 MPa). The primary cause for this degradation was inhomogeneous flow [27]. On the other hand, the rapid cooling rate and residual stresses resulting from a large temperature gradient are known to adversely affect mechanical properties [28].

Mechanical properties reduced as the channel depth increased. Although the increased channel depth increased the volume of the load-bearing joint metal, the load-carrying capacity reduced with increasing channel depth. This was due to the fact that the high and irregular thermal cycles caused by the increased channel depth caused degradation in the microstructure of the material (Fig. 10). More Cu material was reshaped with increased channel depth and higher heat. The sample *S*3 had the highest volume of joint metal and relatively less porosity than the other samples. However, its mechanical properties were lower than those of the samples *S*1 and *S*2. This confirmed that the degradation in mechanical properties depended on the microstructure. It is reported in the literature that porosity is the most important action mechanism in the occurrence of damage [27]. However, the amount of volume reshaped in the study was the most effective variable on mechanical properties.

The behaviours of materials under the heat effect are different; therefore, the optimum channel depth should be determined separately for each material type in order to improve the mechanical properties of the joint. According to the data from the literature, increased heat values improved the mechanical properties in dissimilar material pairs from the materials used in the study [24]. In fact, many metallurgical parameters such as melting temperature during casting, solidification conditions and casting speed are effective on the quality and mechanical properties of Cu. During the recrystallization process of Cu due to thermal cycles and pressure, it is inevitable to change some metallurgical properties and thus mechanical properties. The mechanical values obtained in this study could not be reported by the previous studies in the joining of Cu and steel materials [21]. This revealed that MLM can be used successfully in the joining Cu and AISI 1040 materials. It is considered that analysing the MLM parameters as compatible with each other and together with the physical design parameters would affect the joint quality even more positively.

## 4 CONCLUSION

In this study, Cu and AISI 1040 materials were joined using Mechanical Locking Method. The effect of different values of the channel depth, one of the physical design parameters, on the joint quality was investigated. The results are given below.

(1) Cu and AISI1040 materials were successfully joined using the MLM method. It was determined that the joint quality can be enhanced by making the joining parameters and the design parameters compatible among themselves.

(2) The increase in the channel depth led to an increase in the heat and amount of reshaped material with undesired grain structure.

(3) While the hardness values decreased at the friction interface in the samples *S*1 and *S*2, they increased slightly in the sample *S*3 due to increased heat and pressure values. It was found that the change in hardness values varied depending on thermal cycles and diffusion.

(4) The highest joint strength was found to be 236 MPa in the sample *S*1 with a decrease of 22% compared to the base material. The lowest joint strength (138 MPa) was observed in the sample *S*3 and the increase in the channel depth affected negatively the mechanical properties.

**Acknowledgements**

This study was carried out with the support of the project coded TEKNO-028, funded by the Scientific Research Project Unit of Sivas Cumhuriyet University. The authors thank Sivas Cumhuriyet University for their support.

## 5 REFERENCES

[1] Mercan, S. (2017). *Mechanical Locking Method. Turkish Patent and Trademark Office.*

[2] Hawryluk, M. (2016). Review of selected methods of increasing the life of forging tools in hot die forging processes. *Archives of Civil and Mechanical Engineering*, *16*(4), 845-866. https://doi.org/10.1016/j.acme.2016.06.001

[3] Cardarelli, F. (2008). *Materials Handbook A Concise Desktop Reference.* 2nd ed. Springer, London, 179í183.

[4] Welding Handbook. (1997). *Welding copper and copper alloys.* 3. American Welding Society, Miami, USA, 2í42.

[5] Chang, C. C., Wu, L. H., Shueh, C., Chan, C. K., Shen, I. C., & Kuan, C. K. (2017). Evaluation of microstructure and mechanical properties of dissimilar welding of copper alloy and stainless steel. *The International Journal of Advanced Manufacturing Technology*, *91*, 2217-2224.

[6] Münster, D. & Hirt, G. (2019). Copper clad steel strips produced by a modified twin-roll casting process. *Metals*, *9*(11), 1156. https://doi.org/10.3390/met9111156

[7] Sisodia, R. P. S., Gáspár, M., Sepsi, M., & Mertinger, V. (2021). Comparative evaluation of residual stresses in vacuum electron beam welded high strength steel S960QL and S960M butt joints. *Vacuum*, *184*, 109931. https://doi.org/10.1016/j.vacuum.2020.109931

[8] Liu, G. L., Yang, S. W., Han, W. T., Zhou, L. J., Zhang, M. Q., Ding, J. W. et al. (2018). Microstructural evolution of dissimilar welded joints between reduced-activation ferritic-martensitic steel and 316L stainless steel during the post weld heat treatment. *Materials Sci and Eng: A*, *722*, 182-196. https://doi.org/10.1016/j.msea.2018.03.035

[9] Meitei, R. K. B., Maji, P., Samadhiya, A., Ghosh, S. K., Roy, B. S., Das, A. K. et al. (2018). A study on induction welding of mild steel and copper with flux under applied load condition. *Journal of Manufacturing Processes*, *34*, 435-441. https://doi.org/10.1016/j.jmapro.2018.06.029

[10] Shanjeevi, C., Satish Kumar, S., & Sathiya, P. (2013). Evaluation of mechanical and metallurgical properties of dissimilar materials by friction welding. *Procedia Engineering*, *64*, 1514-1523. https://doi.org/10.1016/j.proeng.2013.09.233

[11] Sahin, M. (2009). Joining of stainless steel and copper materials with friction welding. *Industrial lubrication and tribology.* https://doi.org/10.1108/00368790910988435

[12] Deepak, P., Latheesh, V. M., Sumesh, A., Unnikrishnan, D., & Santhakumari, A. (2018). A finite element analysis of dissimilar materials diffusion bonded joints. *Materials Today: Proceedings*, *5*(5), 12484-12489. https://doi.org/10.1016/j.matpr.2018.02.229

[13] Yao, C., Xu, B., Zhang, X., Huang, J., Fu, J., & Wu, Y. (2009). Interface microstructure and mechanical properties of laser welding copper-steel dissimilar joint. *Optics and Lasers in Engineering*, *47*(7), 807-814. https://doi.org/10.1016/j.optlaseng.2009.02.004

[14] Simoen, B., Faes, K., & De Waele, W. (2017). Investigation of the weldability of copper to steel tubes using the electromagnetic welding process. *International Journal of Sustainable Engineering*, *8*(1), 7-7. https://doi.org/10.21825/scad.v8i1.6811

[15] Tähtinen, S., Laukkanen, A., & Singh, B. N. (2001). Investigations of copper to stainless steel joints. *Fusion Engineering and Design*, *56*, 391-396. https://doi.org/10.1016/S0920-3796(01)00338-6

[16] Zhang, B., Zhao, J., Li, X., & Feng, J. (2014). Electron beam welding of 304 stainless steel to QCr0.8 copper alloy with copper filler wire. *Transactions of Nonferrous Metals Society of China*, *24*(12), 4059-4066. https://doi.org/10.1016/S1003-6326(14)63569-X

[17] Celik, S. & Ersözlü, İ. (2009). Investigation of the mechanical properties and microstructure of friction welded joints between AISI 4140 and AISI 1050 steels. *Materials and Design*, *30*, 970-976. https://doi.org/10.1016/j.matdes.2008.06.070

[18] Ramachandran, K. K., Murugan, N., & Shashi, K. S. (2015). Influence of tool traverse speed on the characteristics of dissimilar friction stir welded aluminium alloy, AA5052 and HSLA steel joints. *Archives of Civil and Mechanical Engineering*, *15*(4), 822-830. https://doi.org/10.1016/j.acme.2015.06.002

[19] Stubbins, J. F., Collins, J., & Min, J. (2000). Evaluation of the deformation fields and bond integrity of Cu/SS joints. *Journal of Nuclear Materials*, *283*, 982-986. https://doi.org/10.1016/S0022-3115(00)00383-4

[20] Chalmers Raymond, E. (2001). The friction welding advantage. *Man Engineering*, *126*(5), 64-64.

[21] Çelik, S. (2012). Microstructure and mechanical properties of friction welding of Copper and AISI 1040 steel. *Electronic Journal of Machine Technologies*, *9*(4), 11-20.

[22] Mercan, S. (2019). Joining of dissimilar metal pairs by mechanical locking method. *Gazi University Journal of Science Part C: Design and Technology*, *7*(1), 25-36. https://doi.org/10.29109/gujsc.437488

[23] Erdem, M. (2015). Investigation of structure and mechanical properties of copper-brass plates joined by friction stir welding. *International Journal of Advanced Manufacturing Technology*, *76*(9), 1583-1592. https://doi.org/10.1007/s00170-014-6387-1

[24] Özkavak, H. V. (2022). Joining Cu30Zn (Brass) and AA6063 alloys using the mechanical locking method. *Russian Journal of Non-Ferrous Metals*, *63*, 560-572. https://doi.org/10.3103/S1067821222050078

[25] Kara, R., Virdil, H., & Çolak, F. (2006). Mechanic of Fe-Cu couple joined by diffusion welding examining the features. *Electronic Journal of Machine Learning Technologies*, *4*, 45-52.

[26] Mercan, S. & Özkavak, V. H. (2022). Joining of AISI 1040 and AA6013 material pairs by mechanical locking method (MLM) using different connection angle. *Journal of the Faculty of Engineering and Architecture of Gazi University*, *37*(4), 2309-2322. https://doi.org/10.17341/gazimmfd.931293

[27] Mercan, S. (2021). Joining dissimilar material pairs by mechanical locking method (MLM). *International Journal of Precision Engineering and Manufacturing*, *22*, 1975-1987. https://doi.org/10.1007/s12541-021-00593-z

[28] Robinson, J. S. & Redington, W. (2015). The influence of alloy composition on residual stresses in heat treated aluminium alloys. *Materials Characterization*, *105*, 47-55. https://doi.org/10.1016/j.matchar.2015.04.01

**Contact information:**

**Serdar MERCAN**, Associate Professor
(Corresponding author)
Sivas Cumhuriyet University, Faculty of Technology,
Mechatronics Engineering Department,
58140, Sivas, Turkey
E-mail: smsmercan@gmail.com

**Arslan KAPTAN**, Assistant Professor
(Corresponding author)
Sivas Cumhuriyet University,
Department of Motor Vehicles and Transportation Technologies,
58140, Sivas, Turkey
E-mail: akaptan@cumhuriyet.edu.tr